Influence of Processing on Ethylene-Propylene Block Copolymers: Structure and Mechanical Behavior

M. Ll. Maspoch, J. Gamez-Perez, E. Gimenez, O. O. Santana, A. Gordillo

Centre Català del Plàstic (UPC), C/ Colom 114, 08222 Terrassa, Barcelona, Spain
Dpt. Tecnología, Universitat Jaume I de Castelló, Campus Riu Sec, 12071 Castelló, Spain

Received 29 October 2003; accepted 5 April 2004
DOI 10.1002/app.20834
Published online in Wiley InterScience (www.interscience.wiley.com).

ABSTRACT: Thin plaques (1, 2, and 3 mm) made of polypropylene homopolymer (iPP) and three ethylene propylene block copolymers (EPBC) with different ethylene content (5.5, 7.4, and 12% in weight) have been obtained by different processing methods (injection molding, injection and annealing, and compression molding). The morphology of the plaques has been studied using polarizing microscopy (PLM), differential scanning calorimetry (DSC), and wide-angle X-ray scattering (WAXS). The results have been related with the mechanical properties of the plaques (MD and TD directions) in tension loading tests. We show the influence of the ethylene content, thickness, and processing method and conditions in the final morphology and how they affect the mechanical behavior. This knowledge can be used to tailor the final properties of a piece. © 2004 Wiley Periodicals, Inc. J Appl Polym Sci 93: 2866–2878, 2004

Key words: polypropylene; block copolymers; injection molding; mechanical properties; structure–properties relations;

INTRODUCTION

Polypropylene is one of the most used commodities polymers because of its good combination of properties (chemical resistance, toughness, and good thermal behavior). However, some disadvantages may limit its use, namely, its poor low-temperature impact strength, surface crazing upon repeated flexing, etc. To solve this problem, several strategies can be found, like blending with different rubbery systems. An alternative way of achieving a good combination of properties, avoiding the problems of dispersion of the phases during processing steps, is by means of block copolymerization. Furthermore, the development of more specific catalyzers allows better control of polymer sequences, which can be tailored to obtain additional advantages, such as improved optical clarity and optimal toughness/stiffness balance.

The aim of this work is the study of the structure and mechanical behavior of several plaques made of polypropylene and three ethylene-propylene block copolymers (EPBC). As polypropylene is known by the great influence of the processing conditions on the final properties of the pieces, especially in the case of injection molding pieces[1–3] or after annealing,[4,5] the present study exams the relationships between the processing induced morphology and the mechanical properties of the plaques. Therefore, plaques in different thickness (ranging from 1 to 3 mm) and processing methods (injection molding, injection molding + annealing, or compression molding) have been obtained and analyzed in structure and tensile behavior.

Correspondence to: M. Ll. Maspoch (maria.lluisa.maspoch@upc.es).

Journal of Applied Polymer Science, Vol. 93, 2866–2878 (2004)
© 2004 Wiley Periodicals, Inc.

EXPERIMENTAL

Materials

Four PP-based materials, one isotactic polypropylene homopolymer (H0) and three EPBC with 5.5, 7.4, and 12% in weight ethylene content (EC), from now on called C1, C2, and C3, respectively, have been employed in this work. The same materials were already the object of previous works of our group.[6,7] The EC of the EPBC was determined by FTIR. The grades were chosen with the most similar melt flow indexes (MFI) available, to use the same processing conditions with all of them. The MFI values determined following the standard ASTM D1238 (230°C/2.16Kg) were: 5.5 (H0), 5.3 (C1), 7.8 (C2), and 8.2 (C3). All the materials were kindly supplied by Basell (Barcelona, Spain).

Processing

The raw materials were received as pellets and processed by a 900 Tm Mateu and Solé injection-molding machine (Barcelona, Spain) to obtain thin plaques of different thickness (t = 1, 2, and 3 mm), as pictured in Figure 1. The barrel temperatures (not considering the feeding zone) ranged from 200 to 230°C, and the tem-

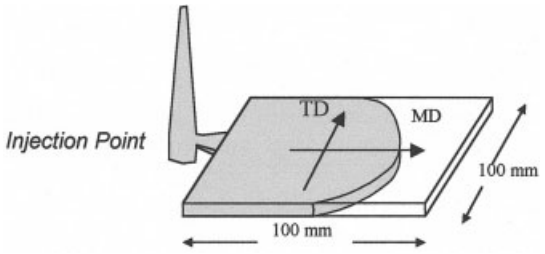

Figure 1 Scheme showing mold geometry. The fan gate thickness at the entrance was t/2.

perature in the nozzle was 250°C. The flow rate in the nozzle was in all cases about 1 cm^3/s. The plaques were allowed to cool inside the mold between 20 and 40 s depending on the thickness of the plaque, and the molds were kept at 28°C by means of a cooling circuit filled with water. The three molds were provided with a fan-gate entrance of thickness half that of the plaque. The plaques were placed at room temperature during at least 48 h before any further operation.

Afterwards, some plaques were subjected to an annealing process at 130°C during 2.5 h. Within this time the annealing was considered complete for all plaques, and it was checked using tension loading fracture tests of deeply double-edged notched tensile (DDENT) specimens. It was observed that 2.5 h of annealing caused a significant variation of the fracture behavior while longer annealing periods, up to 71 h, did not seem to affect any further the response of the materials, indicating an stabilization of the polymer structure. At 100 h of annealing, degradation of the material was perceptible by a clear yellowish color of the plaques.

On the other hand, plaques of all materials were obtained from pellets with a hot plate hydraulic press at 180°C and 45 bars. The dimensions of the plaques were 150 × 150 mm in two nominal thicknesses (1 and 2 mm). According to the processing method, the following code will be assigned to the plaques: Injection molding (IM), Injection and Annealing (IMA), and Compression Molding (CM). The samples will then be named as: material-thickness processing (e.g., "C2–1 mm IMA" represents the plaques of material C2, 1mm thick, obtained by injection molding + annealing). The direction in which the plaques have been tested has been specified as MD or TD (melt flow direction and transversal to melt flow, respectively), as shown in Figure 1.

Structure

As is well known, the structure and properties of injection molded plastic articles are, in general, far from being homogeneous, especially in the case of PP.[8,9] During the injection process, the material enters inside the cooled mold at high pressure through a small gate. This causes the polymer to crystallize under a high shear stress, especially near the surface, as described by the Tadmor's model,[10] resulting in a skin-core processing induced morphology. As this structure is not uniform in all parts of the plaque (depending on the distance from the injection point[11]), and it is of common knowledge that there is a strong relationship between microstructure and final properties of the plastic material, different values of density, hardness, or elastic modulus can be found in different points of the injected plaques. For such a reason, all the morphological characterization has been carried out as close as possible to the center of the injected plaques.

In semicrystalline polymers, the skin/core structure can be observed with the aid of polarizing light microscopy (PLM), since they show different birefringence. Thin slices (20 μm) of the plaques were cut with a fresh razor blade set on a microtome Reichert Jung 2040 (Nussloch, Germany) perpendicular to the MD. After that, they were examined with PLM where clear skin/core structures were observed for all specimens. In literature[1] such a structure is accepted to be composed of highly oriented birenfringent surface layers (skin layers) and a core layer with a broad distribution of spherullites. The skin layer can be described with a shish-kebab model, as shown in Figure 2, where tie

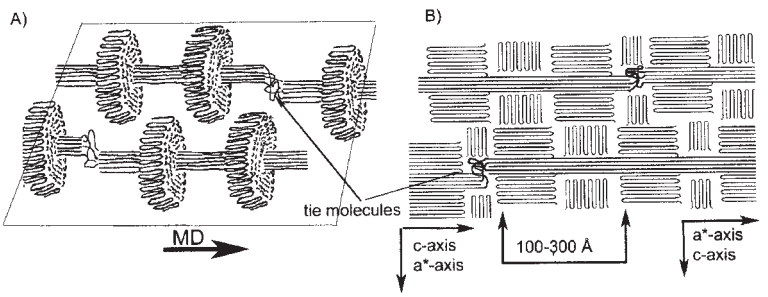

Figure 2 Schema describing the shish-kebab microstructure of the skin, adapted from the literature.[1,2]. (A) Only the structures with their c-axis oriented in MD are shown. (B) Cross-section view from (A).

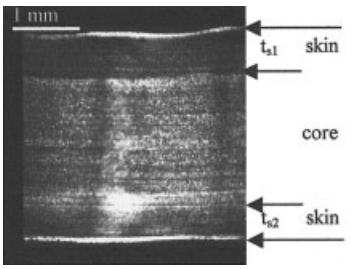

Figure 3 Determination of skin thickness from a photomicrograph (H0–3mm IM).

molecules have been included in the schema as they have a great influence on the mechanical properties.[12] From the PLM images, the thickness of both surfaces was measured and the average value of skin thickness, t_s, was calculated (see Fig. 3.)

$$t_s = (t_{s1} + t_{s2})/2 \quad (1)$$

In an effort to characterize the morphology of the different zones (skin and core), differential scanning calorimetry (DSC) tests from the plaques were carried on. With a fresh razor blade, 10–13 mg specimens were cut from the skin or the core of the injected plaques, using as a guide the PLM images. They were heated (30–200°C at 10°C/min) using a Pyris 1 series calorimeter (Perkin-Elmer, Boston, MA), and the resulting thermograms (heat flow vs. temperature curves) recorded. From the DSC thermograms, the enthalpy of fusion ΔH_f and melting temperature (peak temperature) T_m can be obtained. A crystallinity index χ_d could be determined using as theoretical value for a ΔH_f of a 100% crystalline copolymer (ΔH^o_{copo}). Since such a sample does not exist, it has been proposed to make a rough approximation using a linear law of mixture,[9] intended only as an approximate way to compare the samples among them:

$$\chi_d = \Delta H_f/\Delta H^0_{copo} = \Delta H_f/(\Delta H^0_{PP} \cdot f_{PP} + \Delta H^0_{PE} \cdot f_{PE}) \quad (2)$$

with f_{pp} and f_{pe} being the weight fraction of PP and PE in the sample, respectively. The theoretical ΔH^0_f values were obtained from the literature (ΔH^0_{PP}= 148 J/g and ΔH^0_{PE}= 296 J/g).[13]

Using Wide Angle X-ray Scattering (WAXS) experiments (reflection geometry), another crystallinity index χ_c could be obtained scanning the surface of all plaques, corresponding to the skin zone. Additionally, in the case of the 2 mm thick plaques, after several polishing processes (decreasing the grain size and finishing with silica powder), we analyzed the core zone and also calculated the crystallinity index. The experiments were performed on a Siemens D5000 Twin diffractometer (Siemens, Germany) with a Ni-filtered Cu Ka radiation source (40 kV, 30 mA). The samples were centered in a goniometer and the diffracted intensity was recorded. The incidence angle was coupled with the detector in the range of $3° < 2\theta < 43°$, with a step of 0.03° every 3 s. The curves obtained (after background correction) (Fig. 4) were deconvoluted using a combination of Gaussian and Lorentzian functions. From the deconvoluted curves, the crystallinity (χ_c) was calculated as follows:

$$\chi_c = Sc/(Sc + Sa) \quad (3)$$

where Sc corresponds to the sum of the areas under the crystalline peaks and Sa to the area below the amorphous halo.

Since the orientation that is present in the morphology of the polymer and the β-phase content can play a significant role in the final properties of a specimen,[1,14] two indexes have been determined to measure them:

$$A_{110} = I_{110}/(I_{110} + I_{111} + I_{131+041}) \quad (4)$$

$$\beta^*_{300} = \chi_c \cdot I_{300}/(I_{110} + I_{040} + I_{130} + I_{300}) \quad (5)$$

The intensity scattered by each peak is represented by I_{hkl} (indicating the corresponding crystallographic plane). The A_{110} index is related with the orientation of the α crystallites in the flow direction.[9] The value of this index is 1 for a fully oriented sample; values for isotropic samples have bean obtained from the compression molded plaques ranging from 0.54 to 0.58 depending on the material (see Table I). The β^*_{300} index that we calculate is just the β_{300} index defined by Turner Jones et al.,[15] which is related to the β-phase fraction multiplied by the overall crystallinity index. Doing so, if there are differences in the crystallinity affecting the α-phase, the β^*_{300} index will not be so affected by them. The following example illustrates

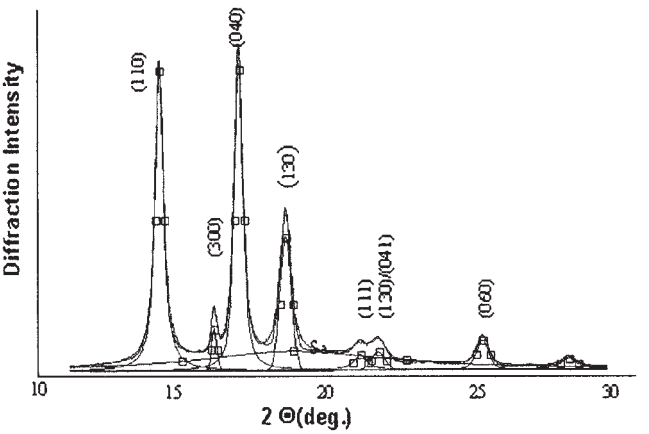

Figure 4 WAXS deconvoluted diffractogram showing position of the corresponding crystallographic planes obtained from the skin of C1–2mm IMA.

TABLE I(A)
Microstructure and Tensile Properties of the H0 and C1 Plaques

		WAXS						DSC	PLM	Tensile		
Material		χ_c	A_{110}	β^*_{300}	$D_{(110)}$	$D_{(130)}$	$D_{(040)}$	χ_d	t_s (μm)		E (MPa)	σ_y (MPa)
H0-1mm CM		0.54	0.56	0.00	192	134	289	0.82	-		1 860	32
H0-1mm IM	core	-	-	-	-	-	-	0.77	249	MD	2 290	35
	skin	0.61	0.96	0.06	195	162	192	0.75		TD	2 220	31
H0-1mm IMA	core	-	-	-	-	-	-	-	276	MD	2 610	40
	skin	0.78	0.97	0.06	235	175	219	-		TD	2 190	33
H0-2mm CM		0.55	0.58	0.00	168	137	191	0.82	-		1 900	32
H0-2mm IM	core	0.53	0.47	0.00	144	135	155	0.77	227	MD	2 070	30
	skin	0.54	0.80	0.06	157	139	174	0.74		TD	1 930	32
H0-2mm IMA	core	0.63	0.49	0.00	170	144	168	-	206	MD	2 080	34
	skin	0.63	0.83	0.05	199	141	190	-		TD	1 970	34
H0-3mm CM		0.55	0.57	0.00	169	148	193	-	-		-	-
H0-3mm IM	core	-	-	-	-	-	-	0.73	196	MD	1 990	32
	skin	0.46	0.58	0.02	143	131	168	0.70		TD	1 900	31
H0-3mm IMA	core	-	-	-	-	-	-	-	168	MD	1 860	33
	skin	0.61	0.66	0.02	174	126	170	-		TD	1 810	33
C1-1mm CM		0.60	0.58	0.00	184	158	197	0.72	-		1 390	25
C1-1mm IM	core	-	-	-	-	-	-	0.59	313	MD	1 880	32
	skin	0.70	0.95	0.08	226	168	217	0.64		TD	1 530	24
C1-1mm IMA	core	-	-	-	-	-	-	0.68	293	MD	1 980	40
	skin	0.76	0.97	0.07	265	185	240	0.76		TD	1 730	28
C1-2mm CM		0.50	0.54	0.00	184	150	203	0.73	-		1 470	24
C1-2mm IM	core	0.55	0.50	0.02	175	165	184	0.63	308	MD	1 430	23
	skin	0.59	0.89	0.06	141	118	138	0.63		TD	1 440	23
C1-2mm IMA	core	0.61	0.41	0.02	161	124	147	0.69	319	MD	1 440	27
	skin	0.70	0.90	0.04	237	173	219	0.70		TD	1 440	26
C1-3mm CM		0.52	0.55	0.00	183	138	187		-		-	-
C1-3mm IM	core	-	-	-	-	-	-	0.62	233	MD	1 320	22
	skin	0.47	0.69	0.06	168	137	180	0.61		TD	1 260	22
C1-3mm IMA	core	-	-	-	-	-	-	0.69	228	MD	1 410	26
	skin	0.62	0.76	0.03	206	137	193	0.67		TD	1 450	26

the advantages of the β^*_{300} index, which will allow us to compare among all samples the presence of β-PP and how it is affected by the processing. A sample of pure β-PP with 10% crystallinity would yield $\beta_{300} = 1$ and $\beta^*_{300} = 0.1$; in the case of another sample with 20% of β-PP and 40% α-PP, the values would be something close to $\beta_{300} = 0.3$ and $\beta^*_{300} = 0.2$. The β^*_{300} index would reveal that there is more β-phase present in the second sample, not being appreciated regarding only the β_{300} index.

Finally, using the Scherrer equation[16] we have calculated the apparent crystallite size ($D_{(hkl)}$) perpendicular to the (110), (040), and (130) crystallographic planes:

$$D_{(hkl)} = \frac{K \cdot \lambda}{\beta \cdot \cos(\theta)} \quad (6)$$

where β is the width at half height in radians of the specific reflection, λ is the wavelength of the radiation used (1.5406 Å), and θ is the position of the peak. The shape factor K has been set as 0.9 (it is an approximate value and the data must be taken as relative).

Tensile properties

Type IV ASTM D-638 tensile specimens were obtained from the plaques to evaluate their response to tension loading in MD and TD. The specimens were mechanized with an Isel Charlyrobot (Cernet, France). The final dimensions were measured prior to tensile tests.

The tension loading tests were performed on a Galdabini universal testing machine (CEAST, Torino, Italy) at 2mm/min and room temperature (23°C), following the ASTM procedure. The Young's modulus (E) and yielding stress (σ_y) were obtained from the engineering stress/strain curves with less than 5% experimental error.

RESULTS AND DISCUSSION

Since the values obtained for all materials and conditions are so extensive, the results are summarized in Table I. To illustrate the most significant trends found within the data, selected diagrams will be presented to complete the text discussions.

TABLE I(B)
Microstructure and Tensile Properties of the C2 and C3 Plaques

		WAXS						DSC	PLM	Tensile		
Material		χ_c	A_{110}	β^*_{300}	$D_{(110)}$	$D_{(130)}$	$D_{(040)}$	χ_d	t_s (μm)		E (MPa)	σ_y (MPa)
C2-1mm CM		0.49	0.52	0.00	170	128	188	0.69	-	-	1 330	19
C2-1mm IM	core	-	-	-	-	-	-	0.53		MD	1520	22
	skin	0.64	0.88	0.04	193	141	189	0.54	148	TD	1310	18
C2-1mm IMA	core	-	-	-	-	-	-	0.57		MD	1760	30
	skin	0.74	0.91	0.03	225	156	207	0.61	161	TD	1550	23
C2-2mm CM		0.49	0.51	0.00	161	125	172	0.64	-	-	1 380	19
C2-2mm IM	core	0.57	0.36	0.00	124	112	169	0.57		MD	1310	20
	skin	0.54	0.74	0.06	184	112	181	0.53	182	TD	1290	19
C2-2mm IMA	core	0.64	0.36	0.00	159	122	134	0.64		MD	1380	22
	skin	0.68	0.76	0.05	228	141	196	0.57	186	TD	1420	22
C2-3mm CM		0.50	0.53	0.00	172	125	190		-		-	-
C2-3mm IM	core	-	-	-	-	-	-	0.58		MD	1190	19
	skin	0.44	0.58	0.05	152	100	167	0.54	220	TD	1220	19
C2-3mm IMA	core	-	-	-	-	-	-	0.59		MD	1330	21
	skin	0.67	0.62	0.06	177	105	172	0.58	207	TD	1360	21
C3-1mm CM		0.47	0.54	0.00	172	139	183	0.56	-		920	12
C3-1mm IM	core	-	-	-	-	-	-	0.51		MD	1370	21
	skin	0.87	0.79	0.03	190	135	193	0.50	130	TD	1210	17
C3-1mm IMA	core	-	-	-	-	-	-	0.57		MD	1550	24
	skin	0.58	0.89	0.03	220	152	205	0.54	131	TD	1310	19
C3-2mm CM		0.46	0.52	0.00	173	137	185	0.58	-		970	12
C3-2mm IM	core	0.47	0.37	0.00	135	118	149	0.50		MD	1150	17
	skin	0.47	0.70	0.03	170	125	180	0.50	232	TD	1050	15
C3-2mm IMA	core	0.51	0.39	0.00	154	122	159	0.57		MD	1230	18
	skin	0.53	0.72	0.04	190	128	188	0.57	229	TD	1260	19
C3-3mm CM		0.47	0.52	0.00	161	132	180	-	-		-	-
C3-3mm IM	core	-	-	-	-	-	-	0.57		MD	1050	15
	skin	0.43	0.58	0.06	153	110	173	0.52	206	TD	1050	16
C3-3mm IMA	core	-	-	-	-	-	-	0.50		MD	1100	17
	skin	0.56	0.64	0.05	187	115	179	0.57	203	TD	1100	17

Structure characterization

Influence of the processing

The observation through PLM of the injected plaques showed a clear skin/core structure (Fig. 5-a). Values of the average skin thickness, t_s, ranging from 130 to 320 microns were obtained among the injected samples. The values obtained when analyzing the annealed plaques showed that there were no significant differences in t_s values (Fig. 5b), proving that the skin/core structure is thermally stable within the current annealing conditions. The plaques obtained by compression molding did not show this type of induced morphology (Fig. 5c).

DSC experiments were performed to characterize the thermal behavior of the skin and core of the plaques for the different processing conditions. The first observation that brings out is the difference among the thermograms obtained for the compression molded and injected plaques (skin and core) as seen in Figure 6. From the curves it can be noticed that the peak temperature of the skin is slightly lower than the one obtained for the core. This difference may be explained by the fact that slower cooling at the core may result in higher crystalline perfection and thus, thicker lamella. In the skin zone, when looking at the model depicted in Figure 2, the fraction with thinner lamella would be the crystallites with their a*-axis

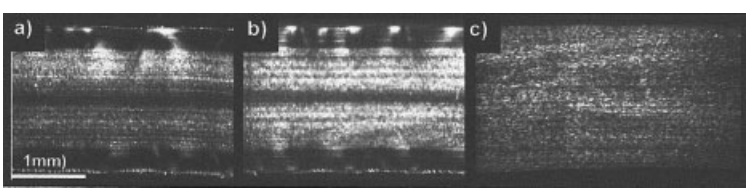

Figure 5 Influence of the processing on the skin/core morphology: (a) C1–2mm IM; (b) C1–2mm IMA; (c) C1–2mm CM.

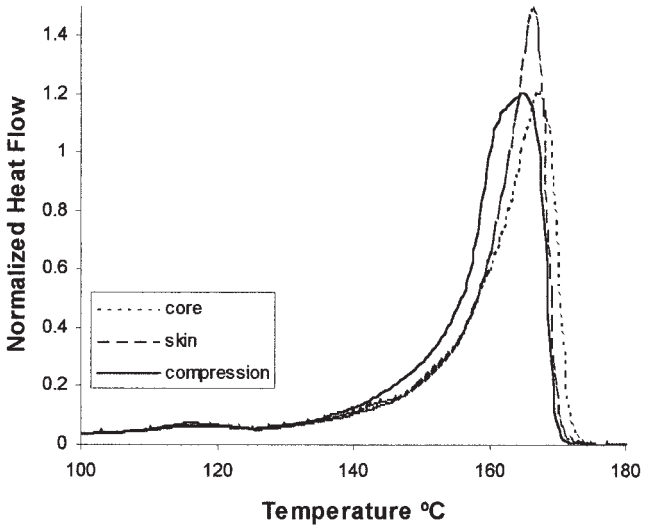

Figure 6 DSC heating thermograms of skin and core layers of C2–2mm IM plaques and C1–2mm CM. Similar results were obtained for all materials.

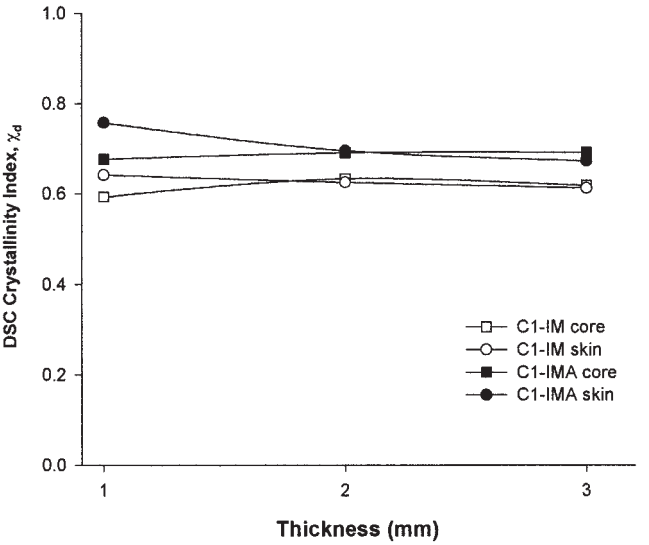

Figure 7 Influence of annealing on the crystallinity (χ_d indexes calculated for C1 IM plaques).

oriented in the MD direction, trapped by the shish-kebab structures.

These results are in agreement with the ones obtained by Fujiyama,[17] even though he found in the skin melting thermogram a tail up to 184°C attributed to the melting of the "shish" structures, not present in ours. It must be pointed out, though, that the dissimilarities can be credited to the differences in viscosity and injection conditions (ours had a higher MFI value and was processed using higher injection temperatures) that can affect the skin formation.[9]

When the thermograms are compared with the corresponding ones for CM, the latter showed lower values of the peak temperature, attributed to the lower temperatures employed during CM.

The crystallinity index obtained by DSC, χ_d, was calculated, and the values obtained for skin and core showed small differences (Table I and Fig. 7). After the annealing process, we noticed an increase in χ_d index in all cases, indicating that secondary crystallization had occurred during annealing (Fig. 7). Similar conclusions can be drawn from the crystallinity indexes obtained by WAX χ_c, which show the same tendencies as in DSC tests.

The orientation of the skin has been measured through the A_{110} index defined by Alberola et al.[4] Here we can find a major influence of the process showing higher values in the IM and IMA plaques than the CM ones, which are supposed to be free of orientation (Fig. 8). The annealing process results in an increase of A_{110}, which indicates that during the secondary crystallization process the amorphous polymer available has been incorporated into the existent crystalline structures already oriented, providing another evidence that the process induced morphology is thermally stable up to 130°C.

The analysis of the WAX diffractograms revealed the presence of some β-phase crystallized polypropylene in the skin of the plaques. No significant traces were found in CM plaques or in the core of the injected ones. The presence of the β-phase is explained by the crystallization under high shear stress close to the mold walls. The β^*_{300} index shows just a slight decrease after annealing. According to this, we can assume that no β-β recrystallization process take place during annealing. This would be in agreement with the thermal history of the plaques, which have been at room temperature (below 100°C[18]) before annealing. Likewise, it is not probable for β-α recrystallization to

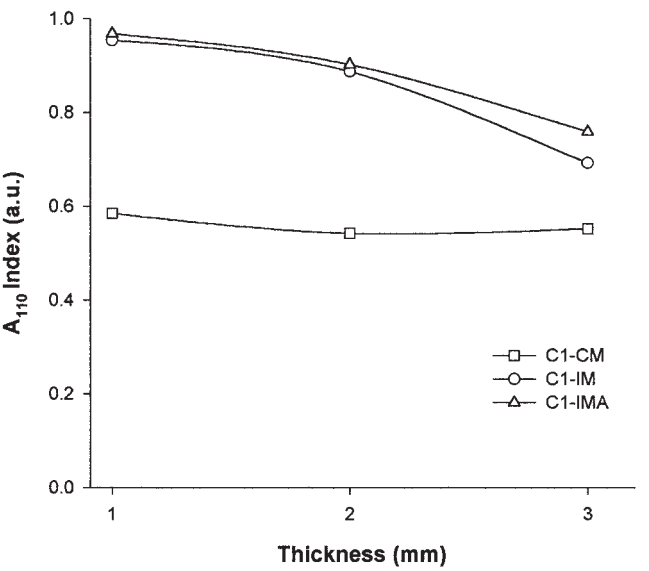

Figure 8 Dependence of A_{110} values (measured on the skin) of material C1 on thickness and processing.

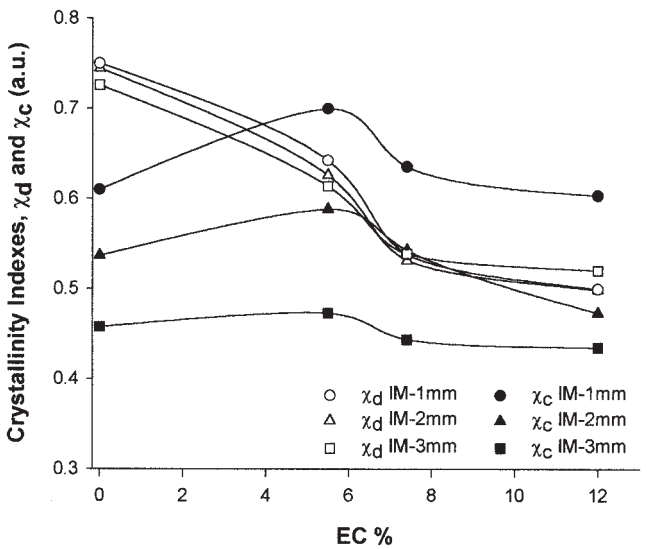

Figure 9 Influence of the EC and thickness on DSC (χ_d) and WAXS (χ_c) crystallinity indexes measured in the skin of the IM plaques.

occur, since the annealing process was carried out at a lower temperature than the melting point of the β-phase, around 145°C. It is suggested then, as a conclusion, that the β-phase crystals are preserved after annealing and some amorphous phase is incorporated into α-phase crystallites, which are furthermore the most stable thermodynamically.

Analyzing the influence of the process on the crystallite size, it can be pointed out that in general, the $D_{(hkl)}$ values follow the trend: CM < IM < IMA, being more noticeable in the 1mm thick plaques. The lower process temperature in CM and the secondary crystallization occurring during annealing are the explanation for this trend, and it is in concordance with the DSC analysis. The annealing step produced an increase in $D_{(hkl)}$ values in the core of the 2 mm injected plaques. The fact that this increase was as high as 15% (the case of the direction perpendicular to the (040) crystallographic plane) shows that the annealing process had affected the inner parts of the plaques and that variation cannot be attributed to experimental scatter. Even though only 2 mm plaques were analyzed, it can be supposed that the annealing affects the core of the plaques injected in the other thickness.

Influence of ethylene content

The evolution of the crystallinity with EC has been followed with the indexes obtained by DSC and WAXS, which are represented in Figure 9 for the IM and IMA plaques, showing that:

1. The values obtained in WAXS and in DSC are not alike but they can be useful to reveal tendencies.
2. In WAXS and DSC experiments it can be noticed that there is a decrease of crystallinity when the EC increases from C1 to C3. In Table I it can be checked that the same tendency is found for the CM plaques.
3. The major disagreement in the tendencies correspond to the values of H0. Such a discrepancy can be justified in the method followed to calculate χ_d, which is based on the value of $\Delta H°$, and this value, when analyzing iPP, can vary in the literature, depending on the method obtained, from 146 J/g to 207 J/g.[18]

On the other hand, the approximation employed by Kalay and Bevis[2] to evaluate the crystallinity among EPBCs has proved to work quite well, keeping in mind that these values are relative and that this approach is not a rigorous one. In Figure 9 the different values of χ_c when the thickness varies can also be noticed, which will be discussed later on.

The values of the average skin thickness (t_s) obtained for the 1 mm injected plaques with different EPBCs are summarized in Figure 10. It can be observed that no straightforward relationships between t_s and the EC can be found, finding a maximum value for C1 (EC 5.5%) and a sharp decrease from C1 to C2 (EC 7.4%).

The evolution of the orientation (A_{110} index) and β-phase content (β^*_{300} index) with the EC shows in general a similar tendency as the average skin thickness of the plaques, as we can see in Figure 10. In the three cases, a relatively sudden drop from C1 to C2 is found.

If we reorder the same data as a function of the MFI (Fig. 11), as an intuitive value that may represent the rheology of the materials, instead of the EC, we can see a decrease of t_s, A_{110}, and β^*_{300} with MFI. The tendencies so found make more sense (more viscosity implies more skin, orientation, and shear stress) and they are in agreement with the results that can be found in literature.[8,9]

Influence of thickness

When the thickness increases for a given material, the evolution of t_s depends on the EC. The plaques injected with lower EC (H0 and C1) present a decrease of t_s with thickness, while the plaques obtained with C2 and C3 exhibit an opposite tendency.

This implies that in the case of the 3 mm plaques, the tendencies found of t_s with MFI are no longer valid. We wondered what could be the main factor affecting this change in properties, and we thought that the crystallization temperature could be the key variable to explain this behavior. It has been shown by several authors that the polyethylene phase can accelerate crystallization in PP-PE blends.[19] Using

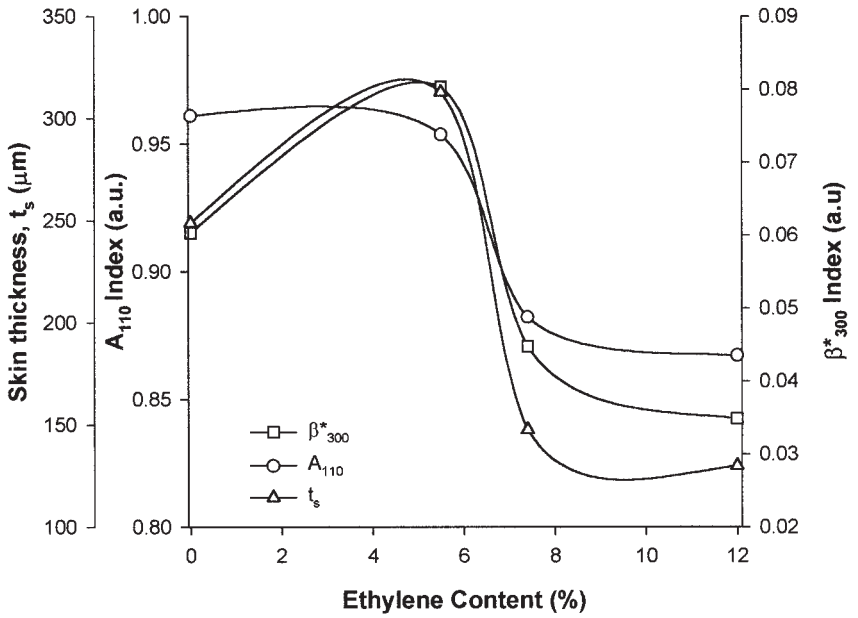

Figure 10 Influence of EC on the skin morphology of 1mm IM plaques.

DSC, we have determined the crystallization temperatures of the four materials. After erasing the thermal history of the samples keeping them 5 min at 210°C, they were cooled down at the rate of 10°C/min (Fig. 12) and the thermograms recorded. The crystallization temperatures, Tc, were determined as the peak temperature in the curve. As a result, we can appreciate that H0 and C1 show a Tc close to 115°C, while C2 and C3 present a much higher Tc (122°C). It seems that only in the case of C2 and C3 is the EC able to promote the crystallization of the PP.

If the values of t_s of the four materials (IM-3mm) are ordered with their Tc, it can be found that, as expected, the materials that crystallize at higher temperature show higher values of t_s (Table I).

As it appears, the skin thickness in the 1 mm plaques is governed by the viscosity of the materials and, in the case of the 3 mm ones, the crystallization temperature presents a major influence (see schema in

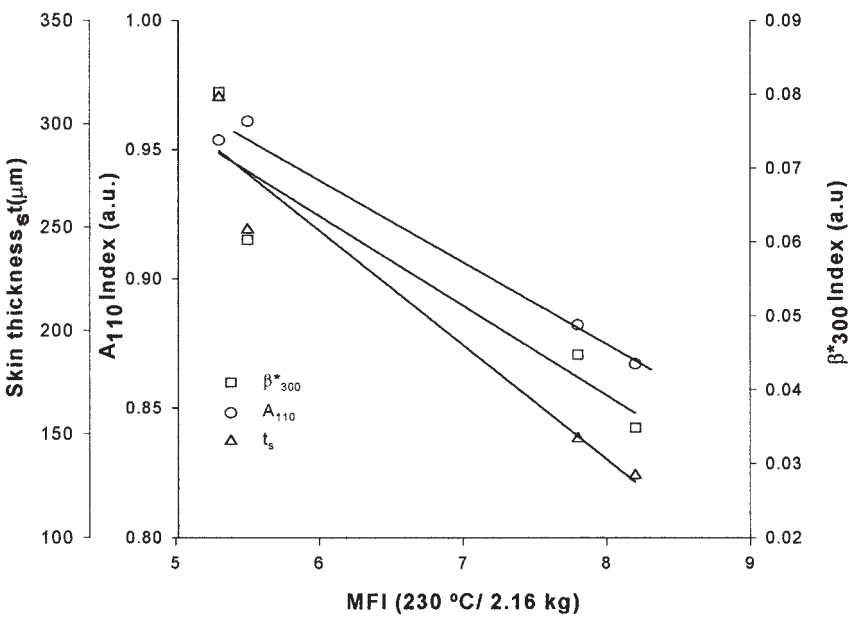

Figure 11 Dependence of the skin morphology parameters of 1mm IM plaques on MFI.

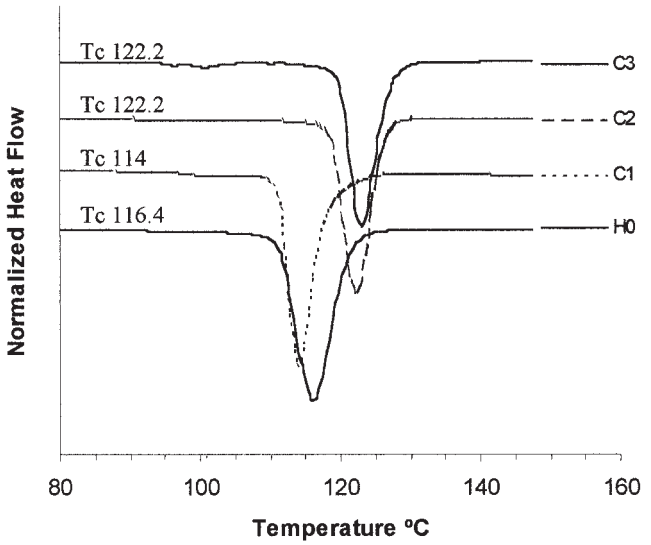

Figure 12 Cooling DSC thermograms for the determination of Tc.

Fig. 13). These different trends can be explained by the differences in the cooling rates. As the polymers are in general bad heat conductors, the thicker plaques take more time to cool down, and the time to crystallize depends more on the Tc. In the 1 mm plaques, the faster cooling masks such dependence, and the influence of the rheological properties of the material is manifested.

Additionally, some other processing variables can have an influence on t_s, like:

Processing conditions. The skin thickness, t_s, will increase with higher shear stress at the solid/melt interface.[9] In our cases, the injection speed was set constant for all geometries and consequently there should be a decrease of the velocity of the injection front as the thickness of the mold increases. As a result, one can expect an increase in the shear stress with thickness and, therefore, also a rise of t_s.

Mold geometry. During cooling of the plaques the heat transfer of the core of the thicker plaques is more difficult, taking more time to cool down allowing the inner chains of the skin to relax. According to the mold geometry, t_s should decrease with the thickness of the plaque. Furthermore, the fan gates are thicker also with the mold, resulting in lower level of shear stress at the entrance.

It can be seen that the overall result cannot be easily predicted since some of the variables act in opposite ways, and it is not the purpose of this work to evaluate quantitatively their influence.

When analyzing the effect of the thickness on crystallinity, we found that the values obtained by WAXS and DSC showed different trends (Fig. 9). The skin crystallinity determined by DSC, represented by χ_d index, does not show any significant variation when the thickness varies; on the other hand, χ_c index determined by WAXS on the skin decreases with an increase in the thickness of the four materials. Apparently, this could lead us to consider that one trend invalidates the other, forcing us to discard one of them. However, if we reflect on the methodology of both techniques, we can arrive at the conclusion that they both may be true. The samples for DSC testing were obtained with a razor blade down to a depth approximately to the measured skin thickness determined by PLM. This means that the samples (about 10 mg) were representative of the whole skin. The WAXS analysis depends on the penetrability of the X-rays, which is less controlled and it can either analyze just the top layer of the skin or induce error from the core region. As a matter of fact, it can distinguish in the "skin" layer of some injected semicrystalline polymers even three layers[20] (amorphous skin, shear layer, and fibrous layer) and also a transition layer between the skin and core, which may present changes in their WAXS spectrum.

For those reasons, we think that although the skin layer presents a reduction of crystallinity determined by WAXS (values of χ_c), this is not representative of the whole zone defined as "skin" by the PLM technique. Hence, we can say that the crystallinity does not really change in the skin with thickness (values of χ_d).

Tensile behavior

It is of common knowledge that processing can have a major influence on the mechanical behavior of materials. Looking at the tensile properties of the plaques processed by the different methods, the following observations can be made:

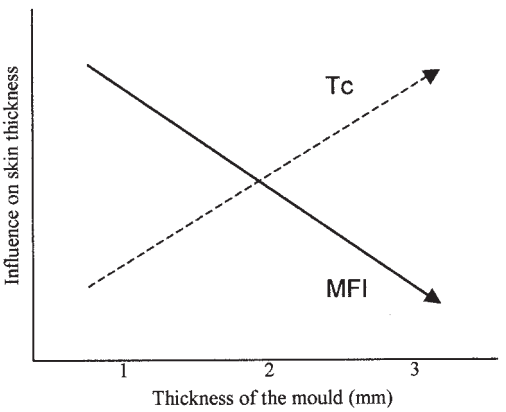

Figure 13 Schema showing the different influence on the skin thickness of the crystallization temperature (Tc) and viscosity (MFI) of the melt, depending on the mold geometry.

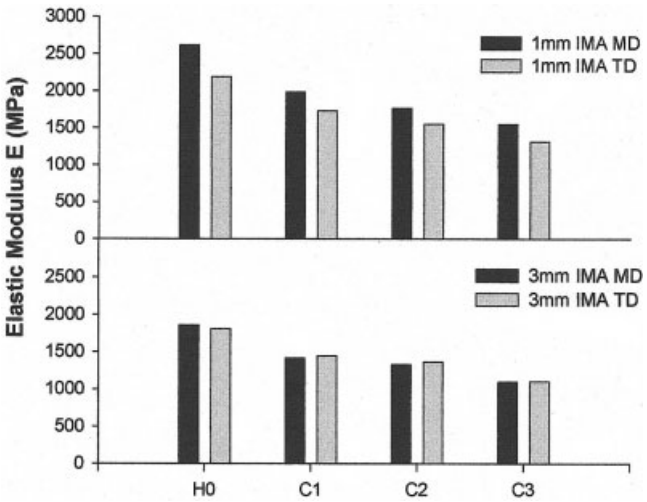

Figure 14 Dependence of the elastic modulus in MD and TD as a function of EC in IMA plaques: (a) 1 mm, and (b) 3 mm thick.

1. The values of E and σ_y obtained for MD and TD in the injected plaques (IM and IMA) are different, indicating that the material presents a preferred orientation. This behavior is not so surprising after the structure characterization, which had already shown that orientation in the skin through the orientation index A_{110} obtained by WAXS. In almost all materials and thicknesses, MD values were higher than TD ones for both E and σ_y (deviations may be attributed to experimental errors). The differences between MD and TD decrease as the thickness of the plaques increase, which is logical considering that the skin fraction decreases, too (Fig. 14).
2. Annealing of the plaques brought as a consequence an increase in the values of E and σ_y with respect to the non annealed (IM). This can be reasoned on the basis of the secondary crystallization that has taken place during annealing. The increase of the crystalline fraction, orientation, and thicker lamella cause a raise in the stiffness of the materials and therefore result in higher tensile properties (Table I) .
3. The ethylene content has a clear influence on the tensile behavior of the plaques, showing a decrease of the properties with an increase of EC in IM, IMA, and CM plaques. This result is explained by two facts: the polyethylene blocks are softer than the polypropylene ones, so the EC reduces the tensile properties; and the reduction of the crystallinity percentage observed with the increase of the EC.
4. When the thickness of the plaques is increased, it can be noticed that E and σ_y in MD decrease while in TD they remain practically constant (Fig. 14). Therefore, the differences between MD and TD values become narrower. Furthermore, the 3 mm plaques present tensile properties that get closer to those obtained for CM. All this indicates that as the plaques are thicker, they present a loss of the preferred orientation in MD. This relationship between orientation and tensile behavior is analyzed in the following paragraphs.

Structure/properties relationship

To study the influence of the structure on the mechanical properties of the plaques, two possible approaches can be followed. One of them is to evaluate the properties of the material as a function of the parameters obtained during structure characterization; and the other method is to consider the skin and core of the plaques as a two-phase composite material, assuming homogeneous properties for the skin and the core.[8] Both approximations have been examined.

As seen in the discussion of the structure of the plaques, when the thickness of the plaques is increased, some morphological changes occur as reflected by the orientation and β-content indexes. To find if there are clear relationships between these parameters and the tensile behavior of the plaques, E and σ_y values have been analyzed with respect to A_{110} and β^*_{300} parameters. We found that:

1. No clear tendency of E nor σ_y with β^*_{300} index can be determined. This may be due to the small amount of β-phase present in our materials (it can be supposed that with much higher content, it would not be masked by other parameters).
2. Both E and σ_y show a correspondence with the orientation index A_{110} in MD. In TD only E displays a slight increases with A_{110}. Such a result seems to be in accordance with the model proposed for the skin, in which the "shish" structures are oriented in MD and not in TD (Fig. 15).

On the other hand, we have already pointed out the problem caused by the penetrability of X-ray radiations in characterizing the skin. So, can the orientation index determined in the surface characterize sufficiently the skin? Apparently, it does; but to consider the skin thickness as a whole, we have reproduced a simple composite model and applied it to our results. This model can be drawn as a set of three strings in parallel (skin/core/skin).[8] The behavior of such a model can be represented by the following equation:

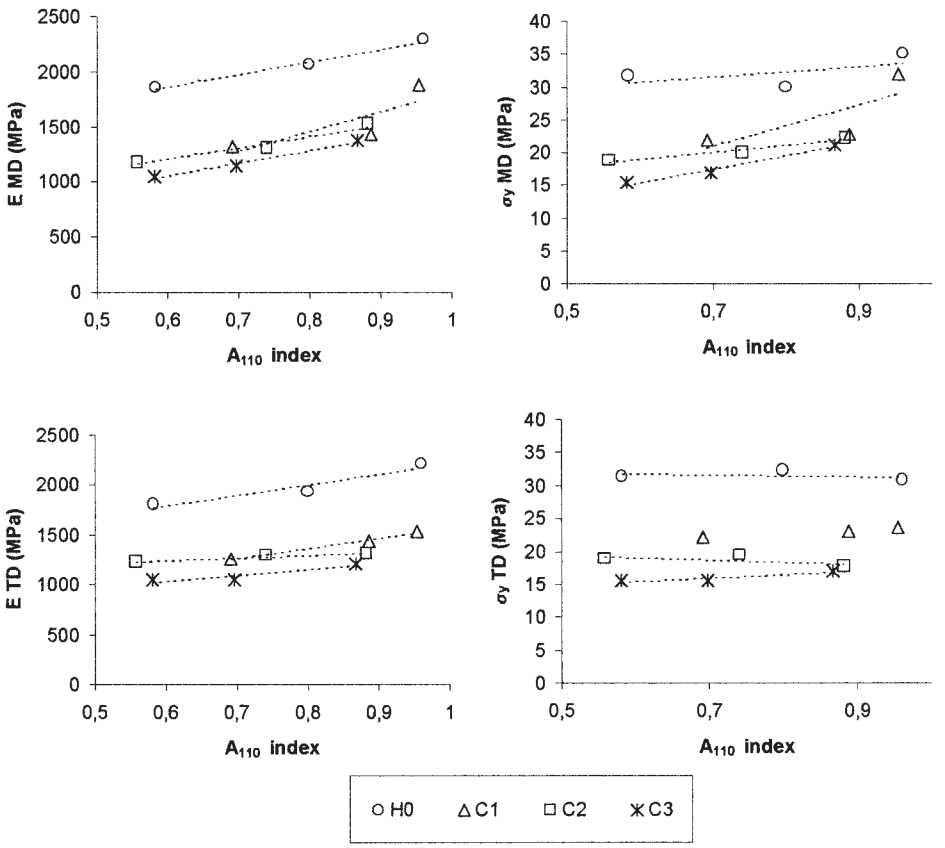

Figure 15 Tensile properties of IM plaques plotted versus A_{110} index.

$$E = \frac{t_{s1} + t_{s2}}{t}(Es - Ec) + Ec \qquad (7)$$

in which the modulus of the plaque is written as a combination of the modulus of the skin (Es) and the core (Ec). Such expression allows us to determine the theoretical modulus of a sample with 100% skin (Es) or 100% core (Ec) by linear regression of the total modulus (E) versus (ts1+ts2)/t. The values obtained with such a simple model must be taken carefully since we assume that there is a common morphology all over the skin and all over the core, which is just a rough approximation.

In Figure 16, it can be observed that the points obtained for the annealed plaques in MD fall quite well in the lines. Similar agreement was found, too, in TD and in the case of the nonannealed plaques. The values obtained for Es and Ec are showed in Table II. The following observations are common to the IM and IMA plaques:

1. The Es values are higher than their corresponding Ec ones in either MD or TD.
2. The Es values in MD are higher than their corresponding ones in TD.
3. The values of Ec in MD and TD do not present strong variations between them.

These trends of Es and Ec justify that in MD, when the thickness increases the tensile properties decrease, since the skin/core ratio decreases (therefore, the

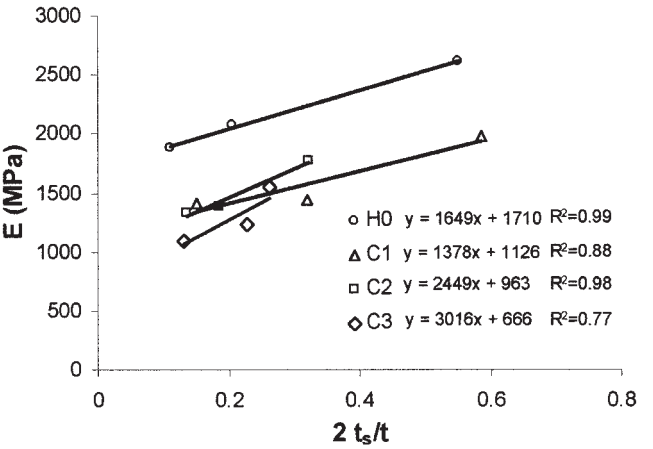

Figure 16 Determination of Es and Ec of the injected and annealed plaques in the MD direction, from linear regressions of E versus $2t_s/t$.

TABLE II
Modulus of the Skin (Es) and Core (Ec) Obtained with the Three String Composite Model

	MD		TD	
	Es (MPa)	Ec (MPa)	Es (MPa)	Ec (MPa)
H0-IM	2860	1760	2780	1670
C1-IM	2330	1100	1750	1220
C2-IM	3070	890	1270	1250
C3-IM	2400	780	1700	900
H0-IMA	3360	1710	2490	1830
C1-IMA	2500	1130	1980	1280
C2-IMA	3410	960	2220	1230
C3-IMA	3680	670	2490	900

weight of the Es decreases, too). In the same way, the Es values obtained in TD are closer to Ec, and this can explain why there is less influence of the thickness on the E values when they are tested in TD.

It has been shown that annealing produces, in general, an increase in E and σ_y. In Table II the variation of the values of Es and Ec after annealing can be seen. The values of Ec remain unchanged, while there is an increase in the values of Es. According to this, one could deduce that the annealing process has only affected the skin of the plaques and not the core. However, the variations of crystallinity and crystallite size had proved that the annealing did affect the whole of the plaques. As a result, we think that annealing affects mainly the tensile properties of the skin, or equally, the oriented skin is mechanically more responsive to annealing.

It can also be remarked that although the differences in Ec values obtained for MD and TD are small (<20%), TD values are always higher than MD ones. This may suggest that the core structure is not as isotropic as previously stated. The values of orientation index obtained in the core of the plaques of 2 mm can corroborate this hypothesis, since they show lower values than the ones obtained with the compression molding ones, which are supposed to be free of orientation.

Despite the fact that the yielding phenomenon happens at the end of the linear tensile behavior, and therefore this model could not apply to σ_y values, the procedure can be repeated using the latter values obtaining similar trends and regression coefficients as in the case of E. Such accord in the results supports the observations made for the modulus.

Finally, from this analysis it can be pointed out that the tensile behavior of the skin of the injected plaques is similar between the EPBCs and iPP. This may suggest that the behavior of the skin of low content EPBCs is governed by the polypropylene induced morphology, which acts as a self-reinforcement. The loss of tensile properties when the ethylene content increases affects mainly the core. This should be taken into account in the design of pieces that require optimum mechanical properties.

CONCLUSION

The final structure of thin plaques obtained with different PP based materials is strongly influenced by the processing, thickness, and ethylene content. The mechanical behavior of the plaques is dependent on the structure, thus affected by the same variables that control structure.

IM processing induced a skin-core structure described on the basis of a model proposed by Fujiyama. Such a model has been very useful to explain the results obtained during the structure characterization. The annealing process has induced an increase in crystallinity and crystalline perfection of the injected plaques, keeping the skin-core structure unaltered, as revealed by PLM, indicating that the latter is thermally stable. On the other hand, the plaques obtained by CM showed an isotropic structure when analyzed with PLM.

With respect to the influence of the ethylene content, it has been observed that a decrease in the crystallinity occurs with an increase of EC. Furthermore, the EC modifies the rheology and crystallization properties of the melt, affecting the skin-core structure of the injected plaques. When the thickness of the injected plaques has increased, a reduction of the orientation parameter can be seen.

It has been verified that some morphological aspects (orientation, β-phase content, etc.) are affected simultaneously by various variables in different ways, increasing the complexity of the study and not being possible in all cases to separate them.

The tensile behavior is explained on the basis of the crystallinity percentage (E and σ_y values increase with crystallinity and crystalline perfection) and degree of orientation in the skin (thinner injected plaques show better tensile behavior than the thick ones). The skin-core structure introduces anisotropy obtaining higher values of tensile parameters when the plaques are tested in the melt flow direction and when they present a higher skin-core ratio. It has been observed that the variations on properties of specimens tested in MD are more pronounced than in the TD direction.

Finally, it can be remarked that the Fujiyama approach of relating the skin-core structure with the tensile properties assuming different values of E for skin and core has proved to be a useful tool in the present study, since it has allowed separating the influence of processing and testing direction on the two main morphologies identified (skin and core).

J. Gamez-Perez is grateful for a doctoral grant from the MCED. The authors thank the MCYT for support in the framework of the project MAT 2000–1112. Thanks are due to

Prof. J. Saura for his welcome in the University Jaume I, Castellon, and to J. Ortega for his aid on the preparation of the samples.

References

1. Fujiyama, M. In Polypropylene, structure and morphology; Karger-Kocsis, J., Ed.; Chapman & Hall: London, 1995; pp. 167–204.
2. Kalay, G.; Bevis, M. J. In Polypropylene, an A-Z Reference; Karger-Kocsis, J., Ed.; Kluwer Publishers: Dordrecht, 1999; pp. 38–46.
3. Karger-Kocsis, J. In Structure Development during Polymer Processing; Cunhaand, A. M.; Fakirov, S., Eds.; Kluwer Academic: Dordrechet, 1999.
4. Alberola, N.; Fugier, M.; Petit, D.; Fillon, B. J of Material Science 1995, 30, 1187.
5. Poussin, L.; Bertin, Y. A.; Parisot, J.; Brassy, C. Polymer 1989, 39, 4261.
6. Ferrer-Balas, D.; Maspoch, M. L.; Martínez, A. B.; Ching, E.; Li, R. K. Y.; Mai, Y.-W. Polymer 2001, 42, 2665.
7. Maspoch, M. L.; Gamez-Perez, J.; Gordillo, A.; Sánchez-Soto, M.; Velasco, J. I. Polymer 2002, 43, 4177.
8. Fujiyama, M.; Kitajima, Y.; Inata, H. J Appl Polym Sci 2002, 84, 2142.
9. Viana, J. C.; Cunha, A. M.; Billon, N. Polymer 2002, 43, 4185.
10. Tadmor, Z. J Appl Polym Sci 1974, 18, 1753.
11. Raab, M.; Kotek, J.; Baldrian, J.; Grellmann, W. J Appl Polym Sci 1998, 69, 2255.
12. Nittaand, K.-H.; Takayanagi, M. J Polym Sci Part B: Polymer Physics 1999, 37, 357.
13. Monasse, B.; Haudin, J. M. Colloid & Polymer Science 1985, 263, 822.
14. Grein, C.; Plummer, C. J. G.; Kausch, H.-H.; Germain, Y.; Béguelin, P. Polymer 2002, 43, 3279.
15. Turner-Jones, A.; Aizlewood, J. M.; Beckett, D. R. Makromol Chem 1964, 75, 134.
16. Alexander, L. E. X-ray Diffraction in Polymer Science; Wiley: New York, 1969.
17. Fujiyama, M.; Masada, I.; Mitani, K. J Appl Polym Sci 2000, 78, 1751.
18. Varga, J. In Polypropylene, structure and morphology; Karger-Kocsis, J., Ed.; Chapman & Hall: London, 1995; pp. 57–115.
19. Utracki, L. A. In Polypropylene, an A-Z Reference; Karger-Kocsis, J., Ed.; Kluwer Publishers: Dordrecht, 1999; pp. 615–620.
20. Schrauwen, B. A. G. Deformation and Failure of Semi-Crystalline Polymers Systems: Influence of Micro and Molecular Structure; Technische Universiteit Eindhoven: Eindhoven, 2003.